Research Article | Vol. 12, No. 12 / 1 Dec 2021 / Biomedical Optics Express 7544
Biomedical Optics EXPRESS

Effect of NIR light on the permeability of the blood-brain barriers in *in vitro* models

TING ZHOU,[1] TYMISH Y. OHULCHANSKYY,[1,2] AND JUNLE QU[1,3]

[1]*Key Laboratory of Optoelectronic Devices and Systems of Ministry of Education and Guangdong Province, College of Physics and Optoelectronic Engineering, Shenzhen University, Shenzhen 518060, China*
[2]*tyo@szu.edu.cn*
[3]*jlqu@szu.edu.cn*

Abstract: The blood-brain barrier (BBB) is a dynamic barrier between the blood microcirculation system and the brain parenchyma, which plays an important role in the pathogenesis of a variety of neurological diseases. Meanwhile, a non-invasive therapeutic approach of photobiomodulation (PBM) has emerged as a promising treatment for neurological disorders through irradiation with near infrared (NIR) light. However, despite multiple encouraging results reported for PBM *in vitro* and *in vivo*, the mechanisms of its therapeutic effect on brain, especially on the BBB, remain barely known. Herein, the effect of NIR light irradiation on the *in vitro* BBB models was studied. 808 nm laser irradiation at the doses of 10 and 30 J/cm^2 was found to significantly increase the permeability of this BBB model. The results showed that NIR light affected mitochondria of cells in the *in vitro* BBB models, leading to an increase in the mitochondrial activity, reactive oxygen species (ROS) level and Ca^{2+} influx. The activity of matrix metalloproteinases and the expression of the tight junction proteins in the endothelial cells were found to be inhibited by the NIR light, resulting in an increase in the BBB permeability. This study suggested a new strategy for drug transport across the BBB in development of treatments for brain disorders.

1. Introduction

The blood-brain barrier (BBB) is a dynamic interface between the peripheral circulation and the central nervous system (CNS). It mainly consists of endothelial cells together with other types of cells, which are connected by tight junction proteins to form a special microenvironment for neuronal function. The BBB protects the brain from various toxins and pathogens, and is critical for normal brain functions [1,2]. Dysfunction of the BBB is often related with the pathogenesis and progression of various brain diseases [3–5]. It also prevents the entry of most drugs into the CNS, making it difficult to develop new treatments for neurological diseases, or new radiopharmaceuticals for brain neuroimaging [6–8]. Thus, the regulation of BBB permeability is expected to become a promising paradigm for therapy of brain disorders.

Recently, photobiomodulation (PBM) has emerged as a promising treatment for various neurological disorders [9–12]. Basically, low level red (~600-700 nm) or near infrared (NIR, 760-1100 nm) light is used in the therapy to preserve, stimulate, and regenerate cells and tissues. Studies have shown that the mechanism of PBM mainly relies on photon absorption in the mitochondria (cytochrome c oxidase), and ion channels in cells, leading to the activation of cell signaling, up-regulation of transcription factors, and increased expression of protective genes [13–15]. Although the BBB plays a crucial role in brain health and disorders, the effect of PBM on the BBB has rarely been studied. Zinchenko et al. reported that 1267 nm laser at 9 J/cm^2 could increase the permeability of BBB and then enhance the beta-amyloid clearance in the mice with Alzheimer's disease [16]. However, there are no studies, which specifically target the molecular mechanisms of the NIR light effect on a BBB using specially designed BBB models.

#438445 https://doi.org/10.1364/BOE.438445
Journal © 2021 Received 27 Jul 2021; revised 22 Oct 2021; accepted 1 Nov 2021; published 12 Nov 2021

Biomedical Optics EXPRESS

Herein, we report the effects of NIR (808 nm) laser irradiation on a *in vitro* BBB model. To determine the effects of the NIR light on the BBB models, we first measured the BBB permeability with transendothelial electrical resistance (TEER). The permeability for various nanoparticles and small molecules was also detected after the irradiation. To figure out the molecular mechanism of the PBM on the BBB permeability, the light effect on cell viability and mitochondial activity were first determined. Reactive oxygen species (ROS) generation, Ca^{2+} level, activity of matrix metalloproteinases (MMPs), and expression levels of related tight junction proteins on the BBB models and their relationship with the BBB permeability were then subsequently determined and analyzed.

2. Material and methods

2.1. Materials

Calcein-AM, Fura-2 AM and the total reactive oxygen species (ROS) assay kit were supplied by Thermo Fisher Scientific (Waltham, MA, USA). Anti-claudin-5 mouse antibody, Anti-occludin rabbit antibody, Alexa Fluor 488 donkey anti-rabbit antibody, Alexa Fluor 488 goat anti-mouse antibody and Alexa Fluor 647 donkey anti-rabbit antibody were purchased from Abcam (Cambridge, England, UK). The MMP-2 and MMP-9 zymography assay kit was obtained from Solarbio Life Sciences (Beijing, China).

2.2. Cell lines

HCMEC/d3 cells (immortalized brain microvascular endothelial cells, BMVECs) and NHA cells (human astrocytes) were cultured at 37 °C, in 5% CO_2 in endothelial medium and DMEM medium, with 10% fetal bovine serum.

2.3. In vitro BBB models

The in vitro BBB models were developed based on BMVECs and NHA cells, according to Mahajan [17,18]. The BBB cell model was growing on a Corning Transwell plate (Corning Incorporated, Corning, NY, USA) containing two compartments permeable Transwell-clear, polyester (PET) membrane inserts (pore size = 3 µm). The inserts were treated with collagan I from rat tail (Thermo Fisher Scientific, Waltham, MA, USA). Then BMVECs were grown on the upper side of the insert and NHA cells were grown on the lower side, as shown in Scheme 1a. The transendothelial electrical resistance (TEER) of the cell models was measured to confirm the formation of an intact BBB. The TEER of the BBB models was measured using an EVOM volt-ohmmeter (World Precision Instruments, Sarasota, FL, USA).

2.4. NIR light irradiation

The irradiation was performed using an 808 nm diode laser. The irradiating power density was 100 mW/cm^2, and the laser doses were adjusted to be 0.3, 1, 3, 10, and 30 J/cm^2 for irradiation. The irradiation parameters are listed in Table 1.

Table 1. The 808 nm laser parameters used during light treatments.

Power density (mW/cm^2)	100	100	100	100	100
Irradiation time (s)	3	10	30	100	300
Laser dose (J/cm^2)	0.3	1	3	10	30

Biomedical Optics EXPRESS

2.5. Cell viability analysis

The *in vitro* BBB models were divided into six groups and irradiated with various laser doses. At 24 h after the irradiation, the BMVECs and astrocytes were separately harvested with trypsin, washed with phosphate-buffered saline and then collected by centrifugation. The cell viability of each type of cell was then assessed by counting the cell numbers with a cell counter *(*Countess II Automated Cell Counter; Invitrogen, Carlsbad, CA, USA.)

For live cell imaging, the control and treated *in vitro* BBB models were stained with Calcein AM and then imaged using a laser scanning confocal microscope.

2.6. Mitochondrial activity analysis

The mitochondrial activity was assessed using an MTT assay and Fluorescence Lifetime Imaging Microscopy (FLIM). The MTT assay is dependent on the mitochondrial activity, because it is a colorimetric reaction catalyzed by succinate dehydrogenase in mitochondrial. Cells cultured in 96-well plates were divided into six groups and irradiated with various irradiation doses. At 4 h and 24 h after the irradiation, MTT was added to each well. Then after 4 h reaction with the cells, the medium was completely replaced with 100 μL dimethyl sulfoxide, and after overnight incubation, the absorbance at 490 nm in each well was measured with a plate reader (Infinite M200, Tecan, Mannedorf, Switzerland).

Two-photon FLIM was implemented using a two-photon excitation laser scanning confocal microscope combined with a time-correlated single photon counting (TCSPC) module. FLIM imaging of cells was performed using two photon excitation at 800 nm and detection in the spectral range of 425-475 nm.

2.7. ROS generation and calcium influx measurement

BMVECs and astrocytes were cultured in 96-well plates and cell dishes. At 24 h after the irradiation, the cells were treated with 2 μM CM-H2DCFDA or 2 μM Fura-2 AM for measurements of ROS generation and Ca^{2+} influx. ROS generation or Ca^{2+} flux in cells was first imaged by a laser scanning confocal microscope.

Then ROS generation and Ca^{2+} flux in cells were separately quantified by measuring the fluorescence at 500 nm and 520 nm using an Infinite M200 plate reader (Tecan).

2.8. MMP-2/9 activity assay

The MMP-2/9 activity of cells was measured using a gelatin zymography assay. After the irradiation, cells were harvested and then lysed with ice-cold lysis buffer (100 mM NaCl, 50 mM Tris-HCl, 0.5% sodium deoxycholate, 1% NP40, 0.1% SDS, 1 mM Na_3VO_4, 1 mM EDTA, 1 μg/mL each of leupeptin and aprotinin, 1 mM NaF, 1 mM phenylmethylsulfonyl fluoride). Then the proteins were then collected by centrifugation at 14, 000 × g for 30 s, at 4 °C. MMP substrates were mixed into 8% and 15% gels, and equal amounts of collected proteins were subjected to SDS-PAGE. After the electrophoresis, Coomassie Brilliant Blue was used for staining the substrates.

2.9. Immunofluorescence

At 24 h after the irradiation, the cells growing on slides were fixed with 4% of paraformaldehyde and then permeabilized with 0.5% of Triton-X 100. A solution of 10% bovine serum albumin (BSA) as blocking agent was incubated with cells for 30 min. The cells were then incubated with the anti-claudin-5 or anti-occludin primary antibodies for 1 h. Next, the Alexa Fluor 488- or Alexa Fluor 637- conjugated secondary antibodies were used for detection. The cells were imaged with a laser scanning confocal microscope, and the fluorescent intensities of 20 representative cells in each group were averaged for quantification.

Biomedical Optics EXPRESS

2.10. Western blot assay

Proteins from cells in each group were collected as described in section 2.8. Equal amounts of proteins from each group were subjected to SDS-PAGE. The proteins were transferred onto PVDF membranes, followed by incubation overnight with primary antibodies to claudin-5, occludin and β-actin at 4 °C. Then the membranes were incubated with the corresponding secondary antibodies for 1 h. The results were presented using a LI-COR Odyssey Infrared Imaging System (Lincoln, NE, USA).

2.11. Statistical methods

Student's t test was used for statistical analysis. The difference between two means was considered to be statistically significant when $p < 0.05$. The results are expressed as the mean ± SD.

3. Results

3.1. BBB permeability increased after the irradiation

The permeability of the *in vitro* BBB model was evaluated using TEER measurements. After 5 days of culturing, the average TEER of the in prepared BBB models was found to increase to more than 200 Ω/cm^2 (Fig. 1). They were then irradiated with the NIR light at laser doses of 0.3, 1, 3, 10, and 30 J/cm^2. At 24 h after the irradiation, the TEER of the treated BBB models was measured to evaluate their permeability. As shown in Fig. 2, the TEER of the NIR irradiated BBB models decreased after the irradiation, when compared with the untreated BBB models, with the most significant decrease at irradiation doses of 10 and 30 J/cm^2. It decreased 19.1% and 15.3%, respectively. Because the TEER was characterized by the integrity of the *in vitro* BBB models, the decrease of TEER indicated that the permeability of the models increased after NIR light treatment. The increase in the permeability for small molecules and nanoparticles confirmed the effect of NIR irradiation on BBB permeability (Fig. S1). In addition, 36 h after the irradiation, the TEER decrease of the BBB models became smaller with time, indicating the increase of the BBB permeability is reversible after the 808 nm light irradiation (Fig. S2).

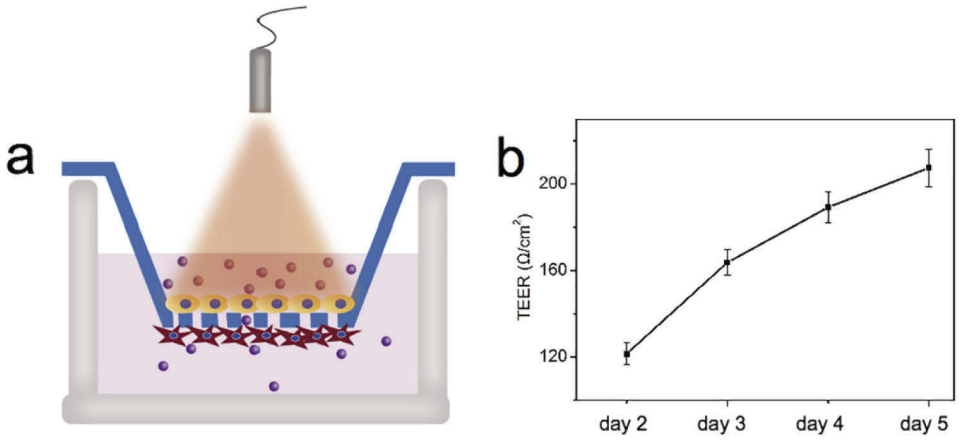

Fig. 1. (a) Scheme of the *in vitro* blood-brain barrier (BBB) model. (b) The transendothelial electrical resistances (TEER) of the BBB models after being cultured for different days.

3.2. Cell viability and mitochondrial activity of the BBB models after the irradiation

Strong NIR light irradiation usually generate local heat, which can cause damage to cells [19]. To verify if the increase of BBB permeability was caused by NIR light- induced cell damage, the

Biomedical Optics EXPRESS

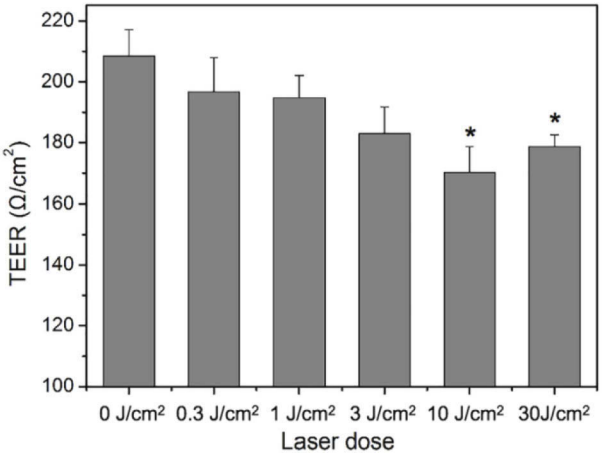

Fig. 2. TEER of the BBB *in vitro* models after irradiation with various laser doses. *P<0.05 versus the untreated group (0 J/cm2). Error bars indicate means ± standard deviation (n=5).

cell viability of cells in the BBB models were tested with a cell counter and live cell imaging. Figure 3 shows that the cell viability of both BMVECs and astrocytes did not changed significantly after the irradiation, indicating that the light doses used in this study did not cause evident cell damage to the BBB models. Thus, the NIR light induced- increases in BBB permeability were not associated with the cell damage. The results in Fig. S3 showed that 808 nm irradiation at 30 J/cm^2 does not cause a noticeable temperature rise in the cell medium, confirming that the increase of BBB permeablity were not caused by the temperature change. (Fig. S3).

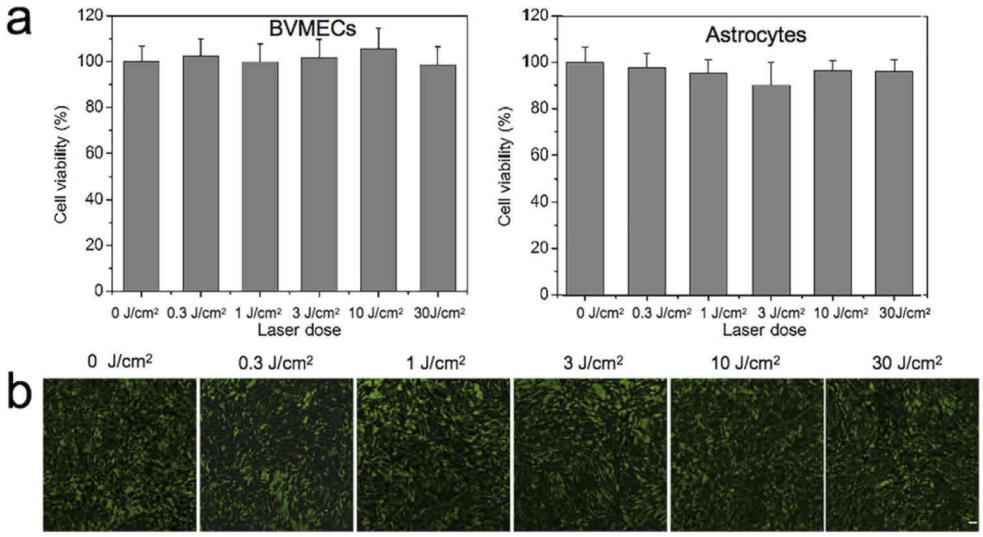

Fig. 3. (a) Cell viability of BVMECs and astrocytes on the BBB models measured by a cell counter after being irradiated at different doses. (b) The cell viability of cells on the BBB models measured with Calcein-AM staining after being irradiated at different doses. Scale bar: 20 μm.

The mitochondrial activity of cells in the BBB models, which was measured 2 h and 24 h after irradiation, rose with an increase in irradiation dose, as shown in Fig. 4. The largest

Biomedical Optics EXPRESS

increase was found for the highest doses of 10 or 30 J/cm^2, which correlated with the data of TEER measurements. These results suggested that NIR light might affect the BBB permeability through mitochondrial activity related- signaling pathways. The mitochondrial activity in the BMVECs after irradiation was also assessed using FLIM of the intracellular NADH (Fig. S4). NADH is a fluorescent coenzyme found in all living cells; its fluorescence lifetime is known to increase several-fold, from 0.3-0.8 ns to 1.0-6.5 ns, upon binding to enzyme partners, which signifies increased ATP production, and stimulation of various biosynthetic pathways [20]. The increase in NADH fluorescence lifetime therefore indicated the promotion of mitochondrial activity in living cells, which could be then visualized using FLIM [21]. In our study, FLIM imaging was performed using two-photon excitation at 800 nm and detection in the spectral range of 425-475 nm, which facilitated FLIM imaging of the two photon excited fluorescence from intracellular NADH [20]. Fig. S4b shows that after the NIR light irradiation at 10 and 30 J/cm^2, the average fluorescence lifetime in the BMVECs increased from 0.97 ns to over 1.6 ns, confirming the promotion of the mitochondrial activities after the NIR irradiation.

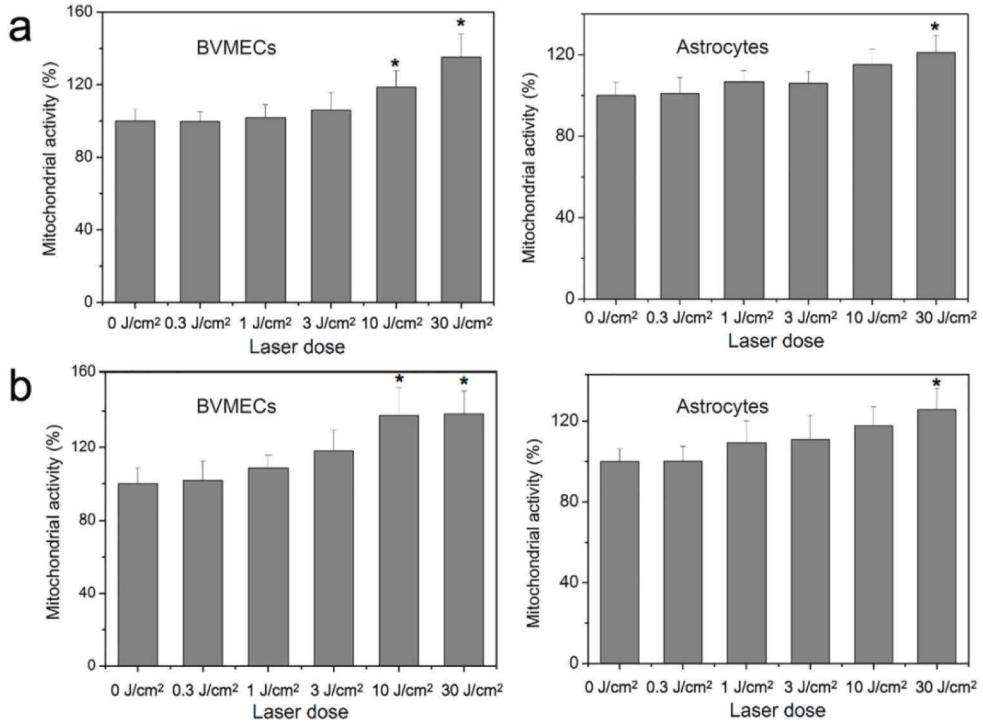

Fig. 4. Mitochondial activity of cells in the in vitro BBB models 2 h (a) and 24 h (b) post irradiation. *P<0.05 versus the untreated group (0 J/cm^2). Error bars indicate means ± standard deviation (n=12).

3.3. *ROS generation and Ca^{2+} flux after the irradiation*

To confirm that irradiation gives rise to the ROS generation and Ca^{2+} infux, we accessed the levels of ROS and Ca^{2+} in BMVECs, astrocytes, and the *in vitro* BBB models, using fluorescence microscopy imaging or measuring the intensity of fluorescence probes. Figure 5 shows that after the NIR light treatment, ROS production in both endothelial cells and astrocytes increased in a dose dependent manners. Compared with that in the control cells, the ROS generation increased by 31.3% and 37.5% in BMVECs, and 49.1% and 50.8% in astrocytes, after the irradiation at 10

Biomedical Optics EXPRESS

and 30 J/cm^2, respectively. In the cells that were a part of the BBB models, the ROS increased even more; it was elevated by 47.5% and 85.6% after irradiation at 10 and 30 J/cm2, respectively. At the same time, the intracellular Ca^{2+} level after the NIR irradiation was found to rose in a similar way (Fig. 6).

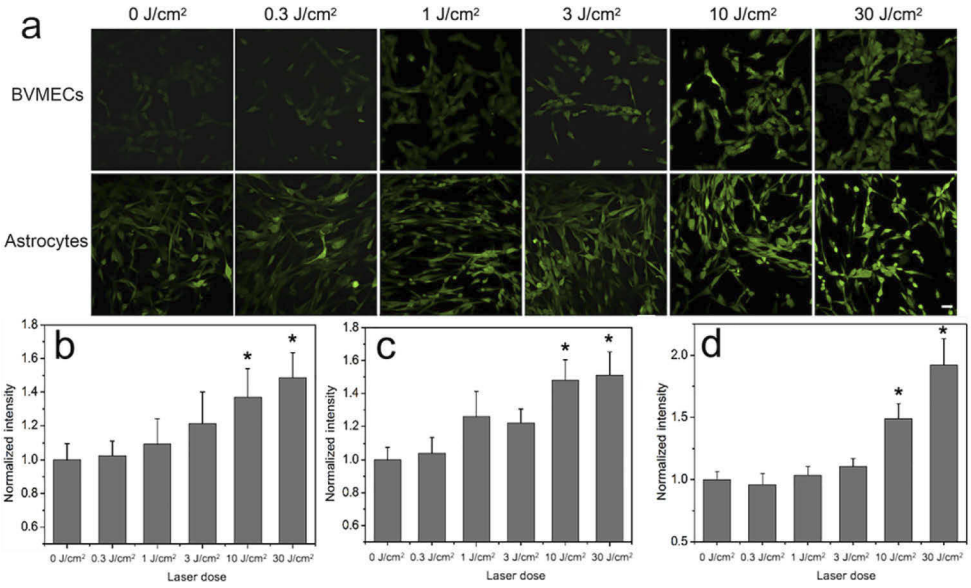

Fig. 5. Light-induced reactive oxygen species (ROS) generation. (a) Fluorescence images shows ROS generation in BVMECs and astrocytes at 10 min after irradiation. Scale bar: 20 μm. Quantification of ROS generation in (b) BVMEC, (c) astrocytes and (d) BBB models at 30 min after irradiation.

Compared with that in the control cells, the ROS generation in cells cultured in dishes increased by 31.3% and 37.5% in BMVECs, and 49.1% and 50.8% in astrocytes, after the irradiation at 10 and 30 J/cm^2, respectively. In the cells that were a part of the BBB models, the ROS increased even more: it was elevated by 47.5% and 85.6% after irradiation at 10 and 30 J/cm^2. At the same time, the intracellular Ca^{2+} level after the NIR irradiation rose in a similar way (Fig. 6).

3.4. MMPs activity after the irradiation

The effect of NIR irradiation on the activity of two prominent MMPs (MMP-2 and MMP-9) in BMVECs was accessed. As expected, the effect of the NIR light on MMPs activity correlated with data on ROS generation; cells irradiated with NIR light at 10 and 30 J/cm^2 showed much higher MMPs activity (Fig. 7(a)). The activity of MMP-2 at these irradiation doses was found to be more than 2.3 and 2.2 fold- higher than those in the untreated cells. Similarly, the activity of MMP-9 was more than 2.0 and 1.9 fold-than those in the untreated cells (Fig. 7(b)).

3.5. Tight junctions proteins expression after the irradiation

TJ proteins are main components of tight junction structure which governs the penetration of molecules through the BBB. A down-regulation of TJ proteins expression is expected to increase the BBB permeability. In particular, Claudin-5 and Occludin are known to be essential TJ proteins that are associated with the MMPs activation causing BBB leakage [29,30]. In our work, we evaluated the expression levels of Claudin-5 and Occludin proteins to further evaluate the effect of NIR light on BBB permeability. The expression of these proteins in the BMVECs cultured in cell dishes (Fig. 8) and as a part of BBB models (Fig. S3) was assessed using

Biomedical Optics EXPRESS

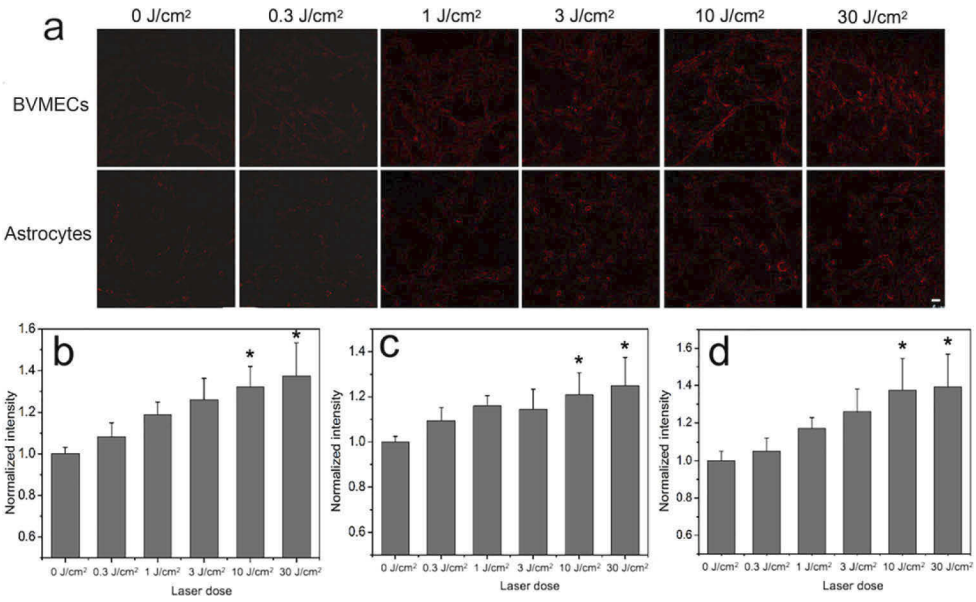

Fig. 6. Light-induced Ca^{2+} levels evaluated with Ca^{2+} fluorescent probe FURA2-AM. (a) Fluorescence microscope images shows Ca^{2+} levels in BVMECs and astrocytes 10 min after irradiation with various laser doses. Scale bar: 20 μm. Quantification of Ca^{2+} changes in (b) BVMECs, (c) astrocytes and (d) BBB models 30 min after irradiation.

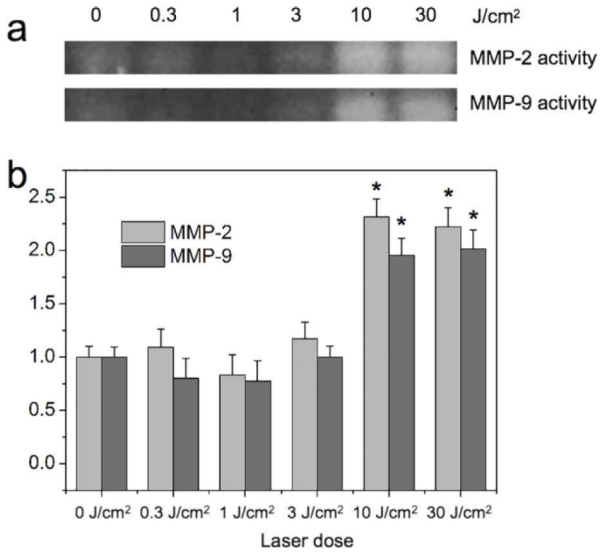

Fig. 7. MMP-2/9 activity of the BBB models after the irradiation. (a) MMP-2/9 activity accessed using the gelatin zymography assay. (b) Quantitative analysis accessed by Image J software. *P<0.05 versus the untreated group (0 J/cm^2). Error bars indicate means ± standard deviation (n=3).

Biomedical Optics EXPRESS

immunofluorescence microscopy imaging and Western blot assay. The results showed that the expression of Claudin-5 and Occludin notably decreased after NIR irradiation at 3, 10 and 30 J/cm^2, while the Claudin-5 expression was significantly reduced after irradiation at 10 and 30 J/cm^2. It should be noted that Claudin-5 and Occludin are transmembrane proteins and are reported to mainly prevent the passage of large molecules [31], which suggests why the BBB permeability after NIR irradiation is enhanced more for nanoparticles than for small molecules (Fig. S1).

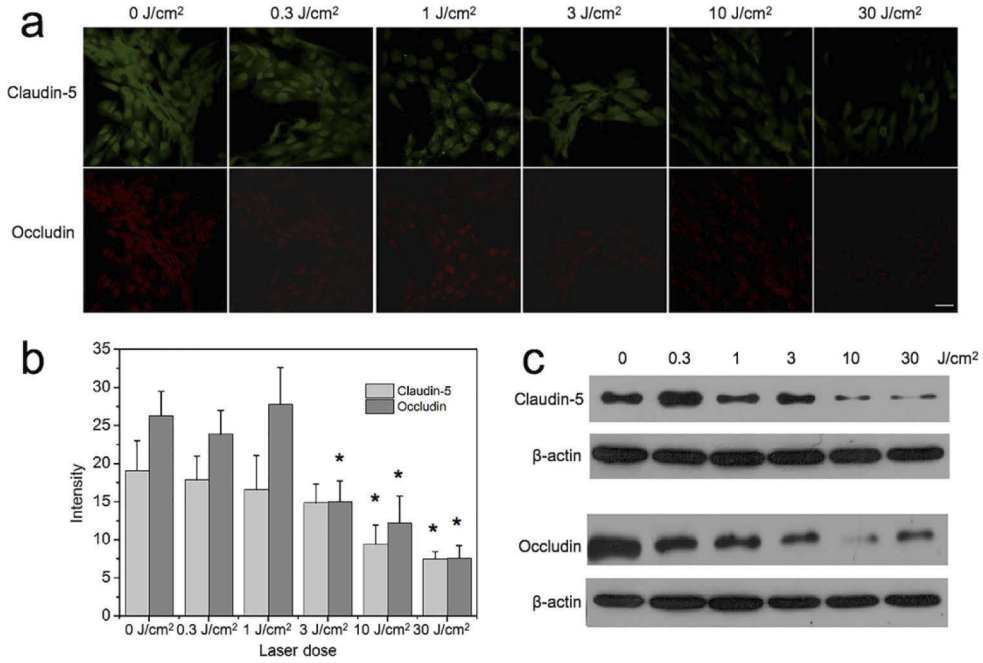

Fig. 8. The expression levels of the tight junction proteins (claudin-5, occludin) on BVMECs after irradiation. (a) Immunofluorescence of claudin-5 and occludin after various treatments. Scale bar: 20 μm. (b) Quantitative analysis of the immunofluorescence performed using Image J software. *P<0.05 versus the untreated group (0 J/cm^2). The fluorescent intensities in 10 random cells from each group were averaged. (c) Expression levels of claudin-5 and occludin assessed by Western blot assays.

TJ proteins are major components of tight junction structures which control the penetration of molecules through the BBB. In our study, we determined the expression levels of claudin-5 and occludin proteins to further evaluate the effect of NIR light on BBB permeability. The expressions of these proteins in the BMVECs cultured in cell dishes (Fig. 8) and as a part of BBB models (Fig. S5) were assessed using immunofluorescence microscopy imaging and Western blot assays. The results showed that the expressions of occludin notably decreased after NIR irradiation at 3, 10 and 30 J/cm^2, while the claudin-5 expression was significantly reduced after irradiation at 10 and 30 J/cm^2. It should be noted that claudin-5 and occludin are transmembrane proteins and are reported to mainly prevent the passage of large molecules [22], which explained why the BBB permeability after NIR irradiation was more enhanced for nanoparticles than for small molecules (Fig. S2).

4. Discussion

Recently, studies have shown that photobiomodulation (PBM) could be used as a promising treatment for various brain disorders. Although the BBB plays a crucial role in brain health and

Biomedical Optics EXPRESS

disorders, the effect of PBM on the BBB has barely been studied. In this study, we analyzed the effects of NIR (808 nm) light irradiation on a *in vitro* BBB model. and explored the mechanisms responsible for the NIR light effects on BBB permeability. After the NIR light irradiation, we found that the TEER of the *in vitro* BBB models decreased and the decrease was significant at the laser doses of 10 and 30 J/cm^2, suggesting the BBB permeability increased after the irradiation. Zinchenko et al. reported that 1267 nm laser at 9 J/cm^2 could also increase the permeability of BBB [16], but the mechanisms remain unknown.

It is commonly accepted that the PBM mechanism is mainly based on promoting mitochondrial activity, thereby affecting the corresponding crucial cell functions [9,14]. In this study, mitochondrial activity of cells in the BBB models rose with an increase in irradiation dose, which suggested that NIR light might affect the BBB permeability through mitochondrial activity related- signaling pathways. Permeability of BBB is regulated by many factors such as tight junction proteins, MMPs, cytokines, ROS, ion channals, etc [23]. Among all these factors, ROS generation and Ca^{2+} flux are closely related to the mitochondrial activity. An increase of ROS production in BMVECs was reported to be responsible for a decrease in TEER, inducing the opening of the BBB [24]. In addition, Ca^{2+} participates in the signaling pathways leading to cytoskeletal alterations in BMVECs. Excessive Ca^{2+} may then cause the BBB compromise [23]. Our previous study demonstrated that 650 nm and 808 nm light irradiation elevated ROS levels and Ca^{2+} flux in different cell lines [25,26]. And in this study, ROS levels and Ca^{2+} flux in the BBB models significantly elevated after the irradiation at 10 and 30 J/cm^2.

MMPs are responsible for the degradation of tight junctions (TJ) proteins in the BBB. And the activation of MMPs was reported to be an important factor which mediated the ROS-induced increase of BBB permeability [27–29]. So next, we measured the activity of two prominent

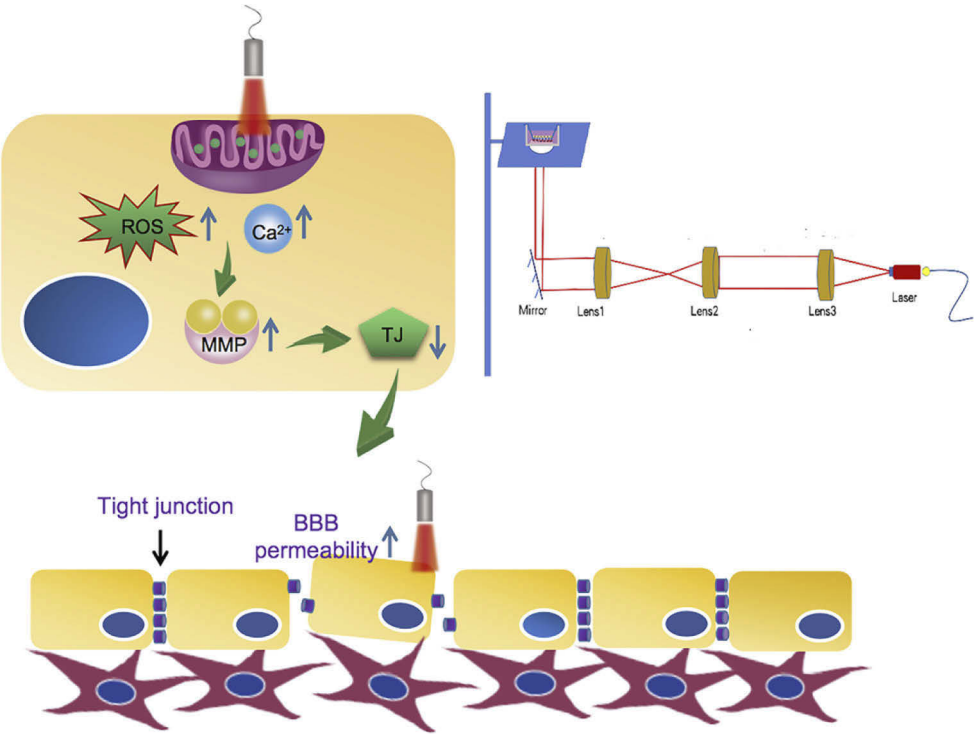

Fig. 9. Scheme of the experiment on the BBB model irradiation and schematic mechanism of the NIR light induced increase of the BBB permeability.

Biomedical Optics EXPRESS

MMPs (MMP-2 and MMP-9) in BMVECs after the irradiation. As expected, cells irradiated with NIR light at 10 and 30 J/cm^2 showed much higher MMPs activity. Then we assume that MMPs were the next factors mediates the increase of BBB permeability by NIR light. Claudin-5 and cccludin are known to be essential TJ proteins that are associated with the MMPs activation, resulting in BBB leakage [30,31]. Down-regulation of their expression is expected to directly lead to the increase of BBB permeability. The results in our study showed that the expressions of claudin-5 and occludin notably decreased after the NIR irradiation at 10 and 30 J/cm^2, confirming that the NIR light induced BBB opening is due to the reduced TJ proteins.

5. Conclusion

In conclusion, the effects of low level NIR light on the *in vitro* BBB models was elucidated in this study. The results indicated that at doses of 10 or 30 J/cm^2, 808 nm laser light can effectively promoted mitochondial activity, following the elevation of ROS generation, Ca^{2+} influx, and the activation of MMPs, leading to the down-regulation of TJ proteins, and consequently increasing the permeability of the BBB models, as illustrated in Fig. 9. Overall, the results of this study should provide new strategies for improving the drug transport across the BBB, for improving treatments of brain diseases.

Funding. National Natural Science Foundation of China (61620106016, 61905153, 61835009, 61875135); Shenzhen Fundamental Research Program (JCYJ20170818090620324); Shenzhen International Cooperation Research Project (GJHZ20180928161811821).

Disclosures. The authors declare no conflicts of interest.

Data availability. Data underlying the results presented in this paper are not publicly available at this time but may be obtained from the authors upon reasonable request.

Supplemental document. See Supplement 1 for supporting content.

References

1. N. J. Abbott, A. A. Patabendige, D. E. Dolman, S. R. Yusof, and D. J. Begley, "Structure and function of the blood-brain barrier," Neurobiol. Dis. **37**(1), 13–25 (2010).
2. D. Richard and P. Alexandre, "The blood-brain barrier," Cold Spring Harb. Perspect. Biol. **7**, a020412 (2015).
3. K. Schoknecht, Y. David, and U. Heinemann, "The blood-brain barrier-gatekeeper to neuronal homeostasis: clinical implications in the setting of stroke," Semin. Cell Dev. Biol. **38**, 35–42 (2015).
4. M. Sweeney, A. Sagare, and B. Zlokovic, "Blood-brain barrier breakdown in Alzheimer disease and other neurodegenerative disorders," Nat. Rev. Neurol. **14**(3), 133–150 (2018).
5. L. Man, Y. Li, L. Zuo, W. Hu, and T. Jiang, "Increase of blood-brain barrier leakage is related to cognitive decline in vascular mild cognitive impairment," BMC Neurol. **21**(1), 159–167 (2021).
6. C. Poon, C. Pellow, and K. Hynynen, "Neutrophil recruitment and leukocyte response following focused ultrasound and microbubble mediated blood-brain barrier treatments," Theranostics **11**(4), 1655–1671 (2021).
7. Rucha Pandit, Liyu Chen, and Jürgen Götz, "The blood-brain barrier: physiology and strategies for drug delivery," Adv. Drug Deliv. Rev. **165**, 1–14 (2021).
8. C. D. Arvanitis, G. B. Ferraro, and R. K. Jain, "The blood-brain barrier and blood-tumour barrier in brain tumours and metastases," Nat. Rev. Cancer **20**(1), 26–41 (2020).
9. P. Cassano, S. R. Petrie, M. R. Hamblin, T. A. Henderson, and D. V. Iosifescu, "Review of transcranial photobiomodulation for major depressive disorder: targeting brain metabolism, inflammation, oxidative stress, and neurogenesis," Neurophotonics **3**(3), 031404 (2016).
10. M. A. Caldieraro, G. Sani, E. Bui, and P. Cassano, "Long-Term Near-Infrared photobiomodulation for anxious depression complicated by Takotsubo cardiomyopathy," J. Clin. Psychopharmacol. **38**(3), 268–270 (2018).
11. D. D. S. Vogel, N. N. Ortiz-Villatoro, N. S. Araújo, M. Jonathas, G. Marques, F. Aimbire, F. A. Scorza, C. A. Scorza and, and R. Albertini, "Transcranial low-level laser therapy in an in vivo model of stroke: Relevance to the brain infarct, microglia activation and neuroinflammation," J. Biophotonics **14**, e202000500 (2021).
12. Z. Ekaterina, N. Nikita, S. Alexander, K. Boris, D. Alexander, S. Elena, A. Arkady, K. Alexander, T. Andrey, M. Aysel, K. Maria, A. Ilana, M. Dmitry, T. Valery, S. G. Oxana, and K. Jurgen, "Transcranial photobiomodulation-induced changes in human brain functional connectivity and network metrics mapped by whole-head functional near-infrared spectroscopy in vivo," Biomed. Opt. Express **10**(8), 4003–4017 (2019).
13. L.F. de Freitas and M. R. Hamblin, "Proposed mechanisms of photobiomodulation or low level light therapy," IEEE J. Select. Topics Quantum Electron. **22**(3), 348–364 (2016).

Biomedical Optics EXPRESS

14. M. Bathini, C. R. Raghushaker, and K. K. Mahato, "The molecular mechanisms of action of photobiomodulation against neurodegenerative diseases: a systematic review," Cell Mol. Neurobiol. **1**, 9 (2020).
15. J. Mitrofanis and L. A. Henderson, "How and why does photobiomodulation change brain activity?" Neural. Regen. Res. **15**(12), 2243–2244 (2020).
16. E. Zinchenko, M. Klimova, A. Mamedova, I. Agranovich, I. Blokhina, T. Antonova, A. Terskov, A. Shirokov, N. Navolokin, A. Morgun, E. Osipova, E. Boytsova, T. Yu, D. Zhu, J. Kurths, and O. Semyachkina-Glushkovskaya, "Photostimulation of extravasation of beta-amyloid through the model of blood-brain barrier," Electronics **9**(6), 1056–1068 (2020).
17. S. D. Mahajan, N. U. Parikh, T. M. Woodruff, J. N. Jarvis, M. Lopez, T. Hennon, P. Cunningham, R. J. Quigg, S. A. Schwartz, and J. J. Alexander, "C5a alters blood–brain barrier integrity in a human in vitro model of systemic lupus erythematosus," Immunology **146**(1), 130–143 (2015).
18. S. D. Mahajan, R. Aalinkeel, D. E. Sykes, J. L. Reynolds, B. Bindukumar, A. Adal, M. Qi, J. Toh, G. Xu, P. N. Prasad, and S. A. Schwartz, "Methamphetamine alters blood brain barrier permeability via the modulation of tight junction expression: implication for HIV-1 neuropathogenesis in the context of drug abuse," Brain Res. **1203**, 133–148 (2008).
19. F. Wetzel, S. Rönicke, K. Müller, M. Gyger, D. Rose, M. Zink, and J. Käs, "Single cell viability and impact of heating by laser absorption," Eur. Biophys. J. **40**(9), 1109–1114 (2011).
20. M. C. Skala, K. M. Riching, A. Gendron-Fitzpatrick, J. Eickhoff, K. W. Eliceiri, J. G . White, and N. Ramanujam, "In vivo multiphoton microscopy of NADH and FAD redox states, fluorescence lifetimes, and cellular morphology in precancerous epithelia," Proc. Natl. Acad. Sci. USA 4(49), 19494–19499 (2007).
21. A. Zbinden, D. A. Carvajal Berrio, M. Urbanczyk, S. L. Layland, M. Bosch, S. Fliri, C. Lu, A. Jeyagaran, P. Loskill, G. P. Duffy, and K. Schenke-Layland, "Fluorescence lifetime metabolic mapping of hypoxia-induced damage in pancreatic pseudo-islets," J. Biophotonics **13**(12), e202000375 (2020).
22. T. Nitta, M. Hata, S. Gotch, Y. Seo, H. Sasaki, N. Hashimoto, H. Furuse, and S. Tsukita, "Size-selective loosening of the blood- brain barrier in claudin-5-deficient mice," J. Cell. Biol. **161**(3), 653–660 (2003).
23. M. M. A. Almutairi, C. Gong, Y. G. Xu, Y. Chang, and H. Shi, "Factors controlling permeability of the blood-brain barrier," Cell. Mol. Life Sci. **73**(1), 57–77 (2016).
24. P. Pun, J. Lu, and S. Moochhala, "Involvement of ROS in BBB dysfunction," Free Radical Research **43**(4), 348–364 (2009).
25. I. Golovynska, S. Golovynskyi, Y. V. Stepanov, L. V. Garmanchuk, L. I. Stepanova, J. Qu, and T. Y. Ohulchanskyy, "Red and near-infrared light induces intracellular Ca^{2+} flux via the activation of glutamate N-methyl-D-aspartate receptors," J. Cell Physiol. **234**(9), 15989–16002 (2019).
26. I. Golovynska, S. Golovynskyi, Y. V. Stepanov, L. I. Stepanova, J. Qu, and T. Y. Ohulchanskyy, "Red and near-infrared light evokes Ca^{2+} influx, endoplasmic reticulum release and membrane depolarization in neurons and cancer cells," Journal of Photochemistry and Photobiology B: Biology **214**, 112088 (2021).
27. V. K. Gupta and CSD , "BBB and MMP-9 elevations: animal experiments versus clinical phenomena in migraine," Expert Review of Neurotherapeutics **9**(11), 1595–1614 (2009).
28. L. Xu, F. Cao, F. Xu, B. He, and Z. Dong, "Bexarotene reduces blood-brain barrier permeability in cerebral ischemia-reperfusion injured rats," PLoS One **10**, e0122744 (2015).
29. A. Bonoiu, S. D. Mahajan, L. Ye, R. Kumar, H. Ding, K. T. Yong, I. Roy, R. Aalinkeel, B. Nair, J. L. Reynolds, D. E. Sykes, M.A. Imperiale, E. J. Bergey, S. A. Schwartz, and P. N. Prasad, "MMP-9 gene silencing by a quantum dot-siRNA nanoplex delivery to maintain the integrity of the blood brain barrier," Brain Res. **1282**, 142–155 (2009).
30. K. Miyazaki, Y. Ohta, M. Nagai, N. Morimoto, T. Kurata, Y. Takehisa, Y. Ikeda, T. Matsuura, and K. Abe, "Disruption of neurovascular unit prior to motor neuron degeneration in amyotrophic lateral sclerosis," J. Neurosci. Res. **89**(5), 718–728 (2011).
31. S. Garbuzova-Davis, D. G. Hernandez-Ontiveros, M. C. Rodrigues, E. Haller, A. Frisina-Deyo, S. Mirtyl, S. Sallot, S. Saporta, C. V. Borlongan, and C. V. Sanberg, "Impaired blood-brain/spinal cord barrier in ALS patients," Brain Res. **1469**, 114–128 (2012).